Hydrodenitrogenation of Quinoline over Carbon-Supported Transition Metal Sulfides

S. EIJSBOUTS,[1] V. H. J. DE BEER, AND R. PRINS[2]

Laboratory for Catalysis, Eindhoven University of Technology, P.O. Box 513, 5600 MB, Eindhoven, The Netherlands

Transition metal sulfide (TMS) catalysts were prepared by impregnation of an activated carbon support with aqueous solutions of first-, second-, and third-row (group V–VIII) transition metal salts, drying and *in situ* sulfidation. The catalysts were tested in the hydrodenitrogenation of quinoline (653 K, 5.5 MPa) in microautoclaves and microflow reactors. The first-row transition metal sulfides had low quinoline conversions to hydrocarbons, and their periodic trend formed a U-shaped curve with a minimum at Mn/C and Fe/C and maxima at V/C and Ni/C. The quinoline conversions to hydrocarbons of the second- and third-row TMS formed volcano curves with maxima at Rh/C and Ir/C and with Mo/C and W/C having the lowest conversions. The transition metal sulfide catalysts with a low quinoline hydrogenation (first-row transition metal sulfides, Mo/C and W/C) also had a low quinoline conversion to hydrocarbons. The transition metal sulfides with the highest quinoline conversions to hydrocarbons (Rh/C, Pd/C, Os/C, Ir/C and Pt/C) had a very high quinoline hydrogenation and a high selectivity for propylcyclohexane. Ru/C and especially Re/C had a good quinoline conversion to hydrocarbons, but also an exceptionally high selectivity for propylbenzene. © 1991 Academic Press, Inc.

INTRODUCTION

The hydrodenitrogenation (HDN) of quinoline (Q) to hydrocarbons is a complex reaction, as indicated in Fig. 1, and it is difficult to unravel the separate steps from a study of the HDN of quinoline alone. Therefore we have also studied the HDN of decahydroquinoline (DHQ) as the key intermediate in the main reaction route of Q–HDN, the HDN of cyclohexylamine (as a substitute for propylcyclohexylamine), and the HDN of *o*-propylaniline (OPA) as the key intermediate in the second route and we published the results in preceding publications (*1, 2*). In the present paper we give a full report of our study of the HDN of quinoline itself using catalysts of carbon-

supported transition metal sulfides (TMS) from the first-, second-, and third-row (group V–VIII) of the Periodic Table. A preliminary account of this work was already published (*3*). Experiments in autoclaves and microflow reactors have been carried out. The autoclaves were used for catalyst screening and they yielded qualitative results. The microflow reactors also enabled us to measure at constant conversion, which makes a comparison of the selectivities of the different catalysts more meaningful.

EXPERIMENTAL

Catalyst preparation and testing in microautoclaves were done as described in the preceding paper (*2*). The reaction mixture contained 4.8 mol% of quinoline and 0.5 mol% of $(CH_3)_2S_2$ in hexadecane (all Janssen Chimica, >99%). All reaction products and intermediates belonging to the main reaction pathways of Q–HDN (Fig. 1) could be identified, albeit only traces of PCHA were
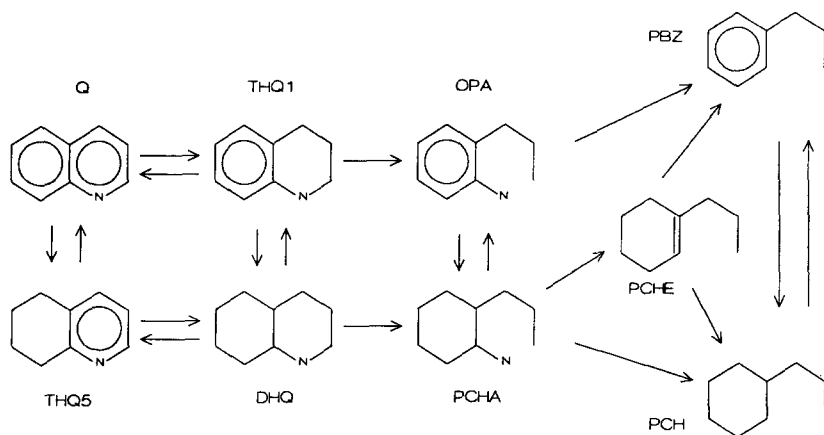
619

FIG. 1. HDN reaction network of quinoline. Q, quinoline; THQ1, 1,2,3,4-tetrahydroquinoline; THQ5, 5,6,7,8-tetrahydroquinoline; DHQ, decahydroquinoline; OPA, o-propylaniline; PCHA, propylcyclohexylamine; PCHE, propylcyclohexene; PBZ, propylbenzene; PCH, propylcyclohexane.

found. Under the given experimental conditions, less than 3 mol% Q was converted to byproducts (cracking and isomerization reactions) which were not taken into account in the further evaluation of the experimental results, i.e., $N_{hc} + N_n + N_{opa} = 100$, in which N_x is the percentage of quinoline converted to compound(s) x.

The microflow experiments were carried out in the gas phase in a high-pressure plug flow reactor. Catalyst, 0.5 g, was diluted with SiC to a total weight of 10 g and sulfided *in situ* (10% H_2S in H_2, 150 std cm^3 min^{-1}). The temperature was increased at 6 K min^{-1} to 643 K and held for 4 h; the pressure was 1.5 MPa. After the sulfidation the pressure was increased to 3 MPa and 12 μl min^{-1} of a liquid feed, consisting of 23.8 mol% quinoline, 3.8 mol% dimethyldisulfide, and 72.4 mol% decane, was premixed with 950 std cm^3 min^{-1} H_2, preheated, and led through the reactor. The products were analyzed every hour with an on-line capillary GC with FID and NPD detectors. When a constant activity was reached after about 18 h on stream the reaction temperature was increased to 663 K and held for 3 h, decreased to 623 K and held for 3 h, and then brought to 643 K and held for 3 h. Thereafter the space velocity was varied in order to

determine the catalyst selectivity over a broad range of HDN conversions. For catalysts with a too high or too low conversion the experiments were repeated with different amounts of catalyst (0.1–1.5 g). Besides the main products (Fig. 1) considerable amounts of byproducts from cracking and isomerization reactions were observed. These byproducts were N-free aromatic or alicyclic C_7 and C_8 hydrocarbons, methyl-propylcyclopentane (C_9), and methylindoles (C_9–N). In the tables representing the experimental results only the sum of all N-free and N-containing byproducts is listed. The reproducibility of the microflow measurements was better than 10%.

RESULTS AND DISCUSSION

Autoclave Experiments

The detailed results of the Q–HDN experiments are listed in Table 1. The Q-conversions to hydrocarbons of the first-row TMS were rather low with Mn/C and Fe/C having the lowest conversions, comparable to that of the pure carbon support. The Q-conversions to hydrocarbons of the second- and third-row TMS were higher than those of the first-row TMS and formed volcano curves with maxima at Rh/C and Ir/C, respectively. These Q–HDN results are in

TABLE 1

HDN of Quinoline in Microautoclaves at 5.5 MPa, 653 K, and $\tau = 0.085$ h · mol Me/mol Q

Catalyst[a]	Product distribution[b]									
	N_{hc}	n_{pch}	n_{pbz}	n_{pche}	N_n	n_{dhq}	n_{thq5}	n_{thq1}	n_q	N_{opa}
C	2	59	15	26	95	2	5	69	24	3
V(4.8)/C	9	61	14	25	80	6	17	68	9	11
Cr(4.9)/C	5	58	17	25	87	3	10	73	14	8
Mn(5.2)/C	4	58	15	27	90	2	10	68	20	6
Fe(5.3)/C	2	51	19	30	95	2	6	55	37	3
Co(5.6)/C	8	60	15	25	86	3	13	52	32	6
Ni(5.6)/C	7	60	15	25	88	3	14	45	38	5
Mo(8.8)/C	14	57	17	26	72	3	14	46	37	14
Ru(9.2)/C	27	68	14	18	66	11	31	42	16	8
Rh(9.3)/C	33	87	7	6	53	7	29	51	13	14
Pd(9.6)/C	29	88	6	6	62	9	25	46	20	10
W(15.5)/C	9	56	15	29	82	3	15	52	30	9
Re(15.7)/C	37	71	12	17	59	16	30	28	26	4
Os(16.0)/C	58	92	5	3	35	4	11	37	48	7
Ir(16.1)/C	71	96	3	1	26	4	7	35	54	3
Pt(16.3)/C	43	94	3	3	43	13	24	50	13	14

Note. $n_{pch} + n_{pbz} + n_{pche}$ = 100
$n_{dhq} + n_{thq5} + n_q + n_{thq1}$ = 100
$N_{hc} + N_n + N_{opa} + N_{by}$ = 100
N_{hc} = conversion.

[a] The wt% of the metals are given within parentheses.

[b] N_x is the Q conversion to compounds x [%], n_x is the selectivity for compound x [%] (N_x/N_{hc} for hydrocarbons and N_x/N_n for double-ring N-compounds).

agreement with results obtained in the HDN of pyridine by carbon-supported TMS. Thus, Ledoux and Djellouli observed a maximum at Ru among the second-row TMS/C catalysts (4), while Vit and Zdražil measured the maximum at Rh (5). The latter authors also found Ir/C to have a higher activity than Pt/C, as well as a higher activity than the second-row TMS/C catalysts, in agreement with our present (Table 1) and former (3) results.

In past years several studies of the behavior of various TMS–HDS catalysts were published. In the high-pressure HDS of dibenzothiophene over bulk TMS a double maximum curve was observed for the first-row TMS and volcano curves for the sec-ond- and third-row TMS with maxima at Ru and Os, respectively (6). Similar trends have been found in the low-pressure HDS of thiophene for carbon-supported TMS (7, 8). The position of the maxima in these thiophene HDS experiments (7, 8) was the same as in our Q–HDN experiments, but, in contrast to HDS, the Q-conversions to hydrocarbons of the third-row TMS (with the exception of W) were much higher than those of the second-row TMS. The correlation between the quinoline and thiophene conversions to hydrocarbons suggests that the catalytic performance of the TMS catalysts in both reactions might be determined by the same type of active sites. However, there is a clear difference between the three rows of

TMS, which might originate in differences between the two test reactions. Under the reaction conditions applied (0.1 MPa) the HDS of thiophene over $NiMo/Al_2O_3$ catalysts proceeds via the hydrogenolysis of the two C–S bonds of thiophene and the formation of H_2S and butadiene, which in turn is converted to butenes and subsequently to butane (9). At high H_2 pressure the hydrogenation to tetrahydrothiophene becomes more important (9–11). The possibility that some highly active TMS catalysts catalyze this reaction pathway even at low pressure cannot be excluded, however. In contrast to HDS, the hydrogenation of the N-containing ring and in most cases also the hydrogenation of the benzene ring of quinoline are necessary steps in the two reaction pathways of Q–HDN via DHQ and OPA (cf. Fig. 1) (11–17). The differences in the hydrogenation activities between various TMS will be more pronounced in the Q–HDN, which requires 8–14 H atoms to convert Q to hydrocarbons, than in the thiophene HDS which strictly needs only 4 H atoms, but may use up to 8 atoms. The differences between the activities for these two reactions might be due to the different activities of the TMS to activate hydrogen which depends on the actual surface electronic structure of the transition metal ion.

Recently Lacroix *et al.* published the activities of several unsupported transition metal sulfides for the hydrogenation of biphenyl at 260°C and 2.2 MPa (18). They observed a maximum at Rh_2S_3 for the second-row TMS and low activities for the first-row TMS. Of the third-row TMS only Hf, W, and Re were studied. Their activities were comparable to those of the corresponding second-row TMS. This biphenyl hydrogenation study indicates that there might also be a reasonable-to-good comparison between the trends of the HDN and hydrogenation activities, which is not surprising given the necessity to hydrogenate the heterocyclic ring before N-removal can occur.

Before discussing the selectivities of the various TMS catalysts it is useful to point out that the compounds present in the reaction product mixture can be divided into several categories with respect to their adsorption properties (14–17). Because of their nonpolar character, the adsorption of the solvent and the hydrocarbon products of the Q–HDN can be neglected compared to the double-ring N-compounds. The aromatic amines (THQ1, THQ5, Q, OPA) have a low basicity due to the interaction of the nitrogen lone-pair electrons with π electrons of the aromatic ring, while the secondary alicyclic amine (DHQ) has a much higher basicity. Its adsorption coefficient was therefore assumed to be twice as large as that of the aromatic amines in the liquid phase (14). By studying the inhibition of the HDS of thiophene by these nitrogen compounds La Vopa and Satterfield (19) could actually measure their adsorption constants. They found the order DHQ $\sim$ THQ5 > Q > THQ1 > ethylaniline (comparable to OPA).

The product distribution within the group of hydrocarbons is dependent on the Q conversion to hydrocarbons (N_{hc}) (Figs. 2, 3) and thus on the position of the TMS in the Periodic System (Fig. 4). All TMS catalysts with low Q-conversions to hydrocarbons (first-row TMS, Mo/C, and W/C) and the pure carbon support had relatively high selectivities for unsaturated hydrocarbons ($n_{pbz} + n_{pche} = 40$–50%). Also the n_{pche}/n_{pch} and n_{pche}/n_{pbz} ratios were rather high for these catalysts and much larger than the thermodynamic equilibrium values determined for gas phase reactions (20). This demonstrates that a large part of the conversion proceeds via the PCHE intermediate. The formation of PCH and PBZ from PCHE was probably limited by the low adsorption of PCHE in the presence of high concentrations of stronger adsorbing double-ring N-compounds. The high selectivity for PCHE was thus not necessarily due to low intrinsic activities of these catalysts to form PCH and PBZ from PCHE. The n_{pch}/n_{pbz} ratios of these low-activity catalysts (Figs. 3, 4) were

FIG. 3. n_{pch}/n_{pbz} selectivity as a function of the conversion of quinoline to hydrocarbons.
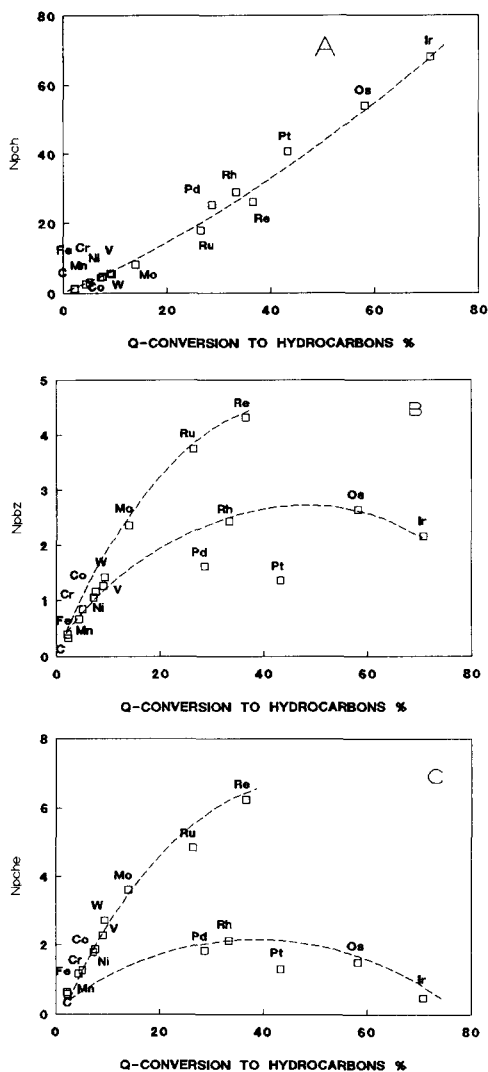

FIG. 2. Plots of the propylcyclohexane (A), propylbenzene (B), and propylcyclohexene (C) selectivities versus the HDN conversion of quinoline to hydrocarbons N_{hc} over carbon-supported transition metal sulfide catalysts.

highly active second- and third-row TMS catalysts (Rh/C, Pd/C, Os/C, Ir/C, Pt/C) had a low selectivity for PBZ and PCHE. These TMS catalysts had high n_{pch}/n_{pche} ratios and some of them also high n_{pbz}/n_{pche} ratios, meaning that the formation of PCH and PBZ from PCHE was rather fast, or that PCH and PBZ were formed directly (without intermediate desorption) from PCHA and OPA. Accordingly, the n_{pch}/n_{pbz} ratios (Figs. 3, 4) were close to the equilibrium ratio of 26 (20). Ru/C and Re/C behaved differently than the other TMS catalysts. Their selectivities for PBZ and PCHE were higher than expected on the basis of their reasonably high Q-conversions (Fig. 2B, 2C). Both catalysts also had a rather low selectivity for OPA (Fig. 5). The low N_{opa} and high selectivity for PBZ are in agreement with the OPA–HDN study of these

much lower than the equilibrium value of 26 (20), indicating that PBZ was formed relatively faster from PCHE than PCH or that in addition PBZ was formed directly from the OPA intermediate. Another possibility is that PBZ and PCH are initially formed through disproportionation: 3 PCHE → 2 PCH + PBZ.
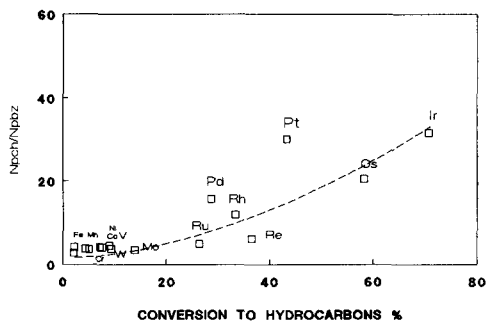
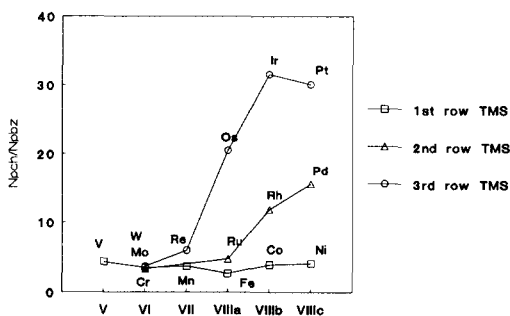In contrast to the first-row TMS, the

FIG. 4. n_{pch}/n_{pbz} selectivity as a function of the position of the transition metals in the Periodic System.
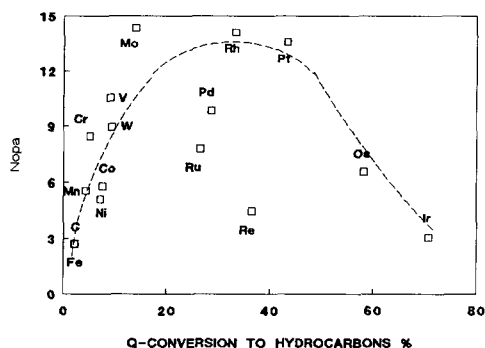
FIG. 5. Conversion of quinoline to o-propylaniline (N_{opa} in percentage) as a function of the quinoline conversion to hydrocarbons, N_{hc} in percentage.

catalysts (2), which indicated that Ru/C and Re/C are highly active in the HDN of OPA and especially that Re/C has a high selectivity to PBZ. In the Q–HDN these catalysts had a relatively high selectivity for PCHE which means that the conversion of PCHA to hydrocarbons over Ru/C and Re/C catalysts proceeds to a large extent via the PCHE intermediate and not via direct hydrogenolysis. Apparently, the further conversion of PCHE to PCH and PBZ was not very fast even though both catalysts had a relatively high N_{hc}. Nevertheless the concentrations of stronger adsorbing N-compounds ($N_n + N_{opa}$) in the reaction product mixture were still appreciable (60–70%). This suggests that the consecutive reactions of PCHE and PBZ only become important at very high Q-conversion to hydrocarbons when $N_n + N_{opa}$ is really low. The high selectivities for PBZ and PCHE found for the Re/C and Ru/C catalysts might also be partly due to their N-product distribution. The Q-conversion to hydrocarbons (N_{hc}) of Re/C was comparable to that of Rh/C and Pt/C, and the N_{hc} of Ru/C to that of Pd/C. Nevertheless, the distributions of the double-ring N-compounds were different (Fig. 6); the main difference being higher DHQ and THQ5 selectivities. DHQ, as the compound with the highest adsorption coefficient from all the compounds in the reaction

product mixture (except for the very reactive PCHA), might lower the PCHE adsorption considerably. On the other hand the differences in N_{dhq} were not that large. The selectivity for PCHE in the DHQ–HDN itself (1, 2) was not high at all for Ru/C and Re/C. Re/C had a high PCHE selectivity in OPA–HDN (2) and the high N_{pche}/N_{hc} of Re/C in Q–HDN thus might come from the OPA reaction pathway. The high PCHE selectivity of the Ru/C catalyst in the Q–HDN, however, had no parallel in the DHQ- and OPA–HDN reactions (1, 2).

For the first-row TMS, N_{opa} changed essentially in the same way as the N_{hc} (Table 1). V/C and Cr/C had a rather high conversion to OPA. With the exception of Fe/C, which had the same N_{opa} as the carbon support, all the first-row TMS were able to catalyze the formation of OPA via the opening of the N-containing ring of THQ1. Just like V/C and Cr/C in the first row of the TMS, Mo/C and W/C had relatively high N_{opa} (Fig. 5), equal to their Q-conversion to hydrocarbons (N_{hc}). Also two of the very active TMS, Rh/C, and Pt/C, had high N_{opa} but in their case the N_{hc} was about twice as high as N_{opa}. A high concentration of OPA at a low (V/C, Cr/C, Mo/C, W/C) or high (Rh/C, Pt/C) N_{hc} demonstrates that the catalyst has a good activity for opening of the N-containing ring, but is not necessarily proof for the (non)ability of the catalyst to convert OPA to hydrocarbons. In our previous publication (2) we showed that when OPA was used as a reactant its denitrogenation was very fast and at 653 K almost as fast as that of DHQ. A high OPA concentration in the Q–HDN is therefore most probably due to the relatively weak adsorption of OPA on the catalyst surface. La Vopa and Satterfield indeed observed a much lower adsorption constant for ethylaniline and aniline than for DHQ, Q, THQ5, and THQ1 (19). In accordance herewith Perot et al. observed that the HDN of anilines is inhibited by Q and THQ1 (21, 22). On the other hand, the low N_{opa} found for some of the highly active
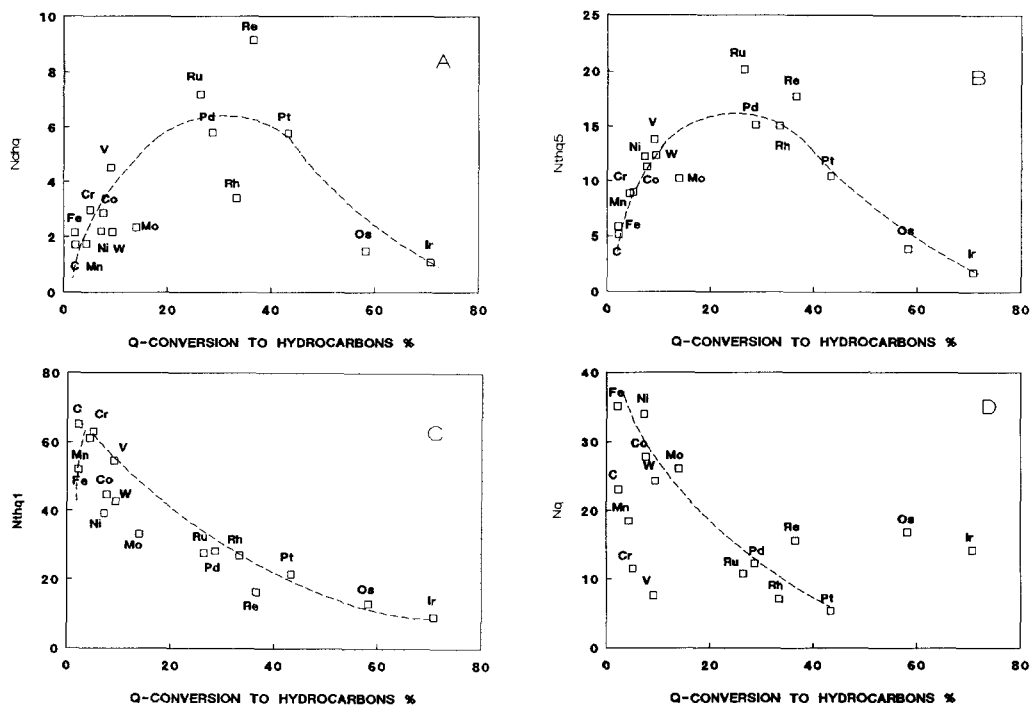
FIG. 6. Conversion of quinoline to decahydroquinoline (A), 5,6,7,8-tetrahydroquinoline (B), 1,2,3,4-tetrahydroquinoline (C), and the residual amount of quinoline (D) as a function of the quinoline conversion to hydrocarbons.

TMS is most probably not due to the low rate of formation of OPA but to its fast conversion to hydrocarbons (Fig. 5) (2).

Also the product distribution of the double-ring N-compounds is determined by the HDN activity which in turn depends on the position of the TMS in the Periodic System (Table 1, Fig. 6). Of the four hydrogenation equilibria (Fig. 1) only the reactions involved in the equilibrium between Q and THQ1 are really fast and the n_q/n_{thq1} ratio might to some extent depend on the cooling rate of the reaction product mixture. The autoclaves were therefore cooled as fast as possible (in 20 min) from 653 K to room temperature. However, due to the insufficiency of the cooling procedure in some cases (C, V/C, Cr/C, Mn/C, Ru/C, Rh/C, Pd/C, and Pt/C) the n_{thq1}/n_q ratio was higher than the equilibrium value of 2 at 653 K (20).

Even with a correction for this effect (by recalculating N_q and N_{thq1} from the measured sum of N_q and N_{thq1}, and the theoretical n_{thq1}/n_q ratio at 653 K), all TMS catalysts had a too low n_{dhq} and a too low n_{dhq}/n_{thq1} ratio compared with the equilibrium values (20) ($n_{dhq} = N_{dhq}/N_n$, in which N_n is the sum of Q, THQ1, THQ5, and DHQ). This is most probably due to the relatively slow formation of DHQ from THQ1. This reaction might even be the rate-determining step of the Q–HDN for some of these catalysts. If one analyzes the results in terms of a THQ1 → DHQ → hydrocarbons consecutive reaction scheme one can read from time-independent plots of the relative concentrations of THQ1 + Q, DHQ, and hydrocarbons (cf. Table 1) against the conversion of THQ1 + Q (as given in many textbooks, e.g., Ref. (23)) that for all catalysts the rate constant

for conversion of DHQ is larger than that for its formation. But at present we cannot judge if for all these catalysts the formation reaction constant is indeed considerably smaller, as needed for a real rate-determining step. Furthermore, it seems that both rate constants change in the same direction when going from one catalyst to the other. Thus the first-row TMS, Mo/C, and W/C have low activities for the reaction to and from DHQ and their Q-conversions to hydrocarbons are low. Os/C and Ir/C apparently had much higher activities for both reactions. Ru/C, Pd/C, Re/C, and Pt/C were intermediate; they had relatively high Q-conversions to hydrocarbons and also relatively high N_{dhq}.

In the same way as the N_{dhq}/N_{thq1} and n_{dhq} ($n_{dhq} = N_{dhq}/N_n$), the n_{thq5} ($n_{thq5} = N_{thq5}/N_n$) of all the catalysts were smaller than the equilibrium ratio, while the n_{thq5}/n_{dhq} ratios were about equal to the equilibrium ratio. This points to a relatively slow hydrogenation of the benzene ring of Q to THQ5, to relatively fast reactions between THQ5 and DHQ and a relatively fast decomposition of DHQ to hydrocarbons. Thus it seems as if for most of our catalysts the hydrogenation of the benzene ring (of Q to THQ5 and of THQ1 to DHQ) is relatively slow and the conversion of DHQ to hydrocarbons is relatively fast. But, again, it is difficult to say whether these benzene ring hydrogenation steps are so much slower that they could be called rate limiting.

In accordance with our conclusion that the hydrogenation reactions are slower than the N-removal reactions in the Q–HDN network, for all TMS/C catalysts the conversion to hydrocarbons was much higher in the HDN of DHQ (2) than in the HDN of Q. In the DHQ–HDN the initial hydrogenation of Q is not required and the TMS catalysts for which one of the hydrogenation steps is rate limiting should have a higher conversion in the DHQ–HDN than in the Q–HDN.

In the literature it has been reported that for Ni–Mo/Al$_2$O$_3$ catalysts the ring-opening reactions of THQ1 and DHQ are rate limit-

ing (11–13). However, this is certainly not true for our TMS/C catalysts. If the ring opening of THQ1 to OPA were rate limiting, then the subsequent reactions of OPA to PCHA and PCHA to hydrocarbons would have been fast and the concentration of OPA should have been very low. Similarly, if the ring opening of DHQ were rate limiting the concentration of DHQ should have been much larger. The fact that the ring-opening reactions and not the hydrogenation of the benzene ring in Q and THQ1 are rate limiting for Ni–Mo/Al$_2$O$_3$ must be due to the high hydrogenation activity of the "Ni–Mo–S" phase. Apparently, the N-removal has not been able to keep up with this high hydrogenation activity.

The results of the present study demonstrate the importance of the TMS in the hydrotreating reactions. With the exception of Fe/C and Mn/C, all the TMS including those with very low Q-conversion to hydrocarbons were able to catalyze all the reaction steps of the Q–HDN mechanism without the assistance of the polar groups (24) of the Al$_2$O$_3$-support. The trends for the HDN activities of the TMS catalysts in the Q–HDN and in the reactions that form part of its reaction network were very much alike. When the initial hydrogenation steps were taken away as in the DHQ–HDN the general trend remained essentially unchanged (2). When the ring opening was eliminated too (CHA–HDN and OPA–HDN) the HDN activity increased strongly but again the periodic trends did not really change (2). Although the ring-opening reaction is considered to be the rate-limiting step of the Q–HDN reaction over Ni–Mo/ Al$_2$O$_3$ catalysts (11–13), our experiments have shown that for the TMS/C catalysts, not the ring opening but the formation of DHQ by the hydrogenation of Q is the slowest step. The CHA–HDN experiments (2) have shown that the trends for the HDN activities remain unchanged even if both slow steps (hydrogenation and ring opening) were removed, the cleavage of the C–N bond in CHA definitely being a fast reaction.

TABLE 2

HDN of Quinoline in a Flow Reactor at 643 K, 3 MPa, and W/F = 0.1 h · mol Me/mol Q

Catalyst	N_{hc}	N_{opa}	N_n	N_{byN}	N_{byHC}
V/C	2	2	94	1	1
Cr/C	2	1	96	1	0
Mn/C	2	1	96	2	0
Fe/C	1	1	94	3	0
Co/C	2	1	94	3	1
Ni/C	2	1	92	4	1
Mo/C	2	2	94	1	1
Ru/C	12	4	78	5	0
Rh/C	79	2	11	6	2
Pd/C	7	1	89	2	1
W/C	5	4	87	3	1
Re/C	11	3	82	3	1
Os/C	88	6	2	1	2
Ir/C	95	1	0	1	2
Pt/C	94	0	3	2	2

This means that all reactions follow the same periodic trends.

Flow Reactor Experiments

Since the catalyst selectivities depend on the activities a comparison of the selectivities of the TMS catalysts can only be properly made at the same conversion to hydrocarbons. However, the large variation in catalyst activity made it impossible to obtain data of the TMS catalysts at the same conversion level from the Q–HDN experiments in the autoclaves. Therefore experiments in a micro-plug-flow reactor were carried out. By varying the gas and liquid space velocity and the amount of catalyst, data could be obtained at the same conversion level for most catalysts. The results of flow experiments under our standard conditions (643 K, 3 MPa, 0.5 g catalyst (0.1 at Me · nm^{-2}) diluted with 9.5 g SiC and W/F = 0.1 h · mol Me/mol Q) are presented in Table 2. The first-row TMS had very low HDN conversions which formed a flat U-shaped curve with a minimum at Fe/C when plotted against the periodic position of the TMS

(Fig. 7). Also in agreement with the Q–HDN autoclave results, the HDN conversions of the second-row TMS followed a volcano curve with maximum at the Rh/C catalyst. The differences between the Rh/C and the other second-row TMS catalysts were much more prominent in the flow experiments than in the autoclave experiments. The HDN conversions to hydrocarbons of the third-row TMS followed a volcano curve with maximum at Ir/C, just like in the autoclave experiments, although the Os/C and Pt/C catalysts had very high HDN conversions too (Fig. 7). Apparently the conversions for these three catalysts were too high to clearly distinguish differences in activity. The W/C and Re/C catalysts had low conversions and the difference between their HDN conversions and those of the high activity third-row TMS/C catalysts was much larger than in the autoclave experiments, just as for the second-row TMS.

The differences between the trends in the gas phase flow reactions and the liquid phase batch reactions must be primarily due to differences in the adsorption coefficients, to the H_2S/H_2 ratios, and/or to the time elapsed before performing the measurements. The relative adsorption coefficients of the reactants and intermediate products are completely different in the liquid and gas phase. For instance, the adsorption coefficient of DHQ is twice as large as those of
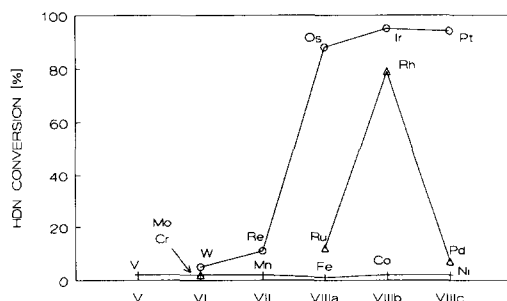

FIG. 7. Periodic trends of the conversions of quinoline to hydrocarbons (N_{hc} in percentage) over carbon-supported transition metal sulfides as measured in a microflow reactor.

TABLE 3

HDN of Quinoline in a Flow Reactor at 643 K, 3 MPa, and Variable Space Velocity

Catalyst	$\frac{W^a}{F}$	n_{pch}	n_{pbz}	n_{pche}	n_{dhq}	n_{thq5}	n_q	n_{thq1}	N_{opa}	N_{by}
				10% HDN conversion						
V/C	2.5	67	16	17	7	32	14	48	7	3
Cr/C	2.6	66	17	17	8	43	12	37	5	4
Mn/C	25	63	23	14	4	32	47	18	3	4
Fe/C	7	64	24	12	5	35	43	18	4	17
Co/C	12.5	76	14	10	11	42	20	27	4	14
Ni/C	12.5	80	12	8	14	46	8	32	4	14
Mo/C	0.3	66	15	20	10	34	18	38	8	7
Ru/C	0.4	78	11	11	19	38	15	28	4	5
Pd/C	0.8	88	7	5	14	55	9	22	2	4
W/C	1	68	12	20	8	40	17	35	11	10
Re/C	0.5	72	14	14	19	48	9	24	3	4
				50% HDN conversion						
W/C	7.1	83	10	7	20	48	11	21	15	23
Re/C	2.1	87	10	3	26	49	8	17	4	15
Os/C	0.3	93	5	3	20	43	19	18	18	4

[a] 10^{-3} W/F in h · g cat/mol Q.

Q, THQ1, and THQ5 in the liquid phase, but six times larger in the gas phase (12, 14, 17). The H_2S/H_2 ratio during the autoclave experiments was 2.5×10^{-3} and 1.5×10^{-4} during the flow experiments. This difference might have led to slightly altered catalyst surfaces and thus to altered activities and selectivities. It is known that an increase in the H_2S/H_2 ratio may lead to an increase in NH_3 removal, but a decrease in hydrogenation (14, 16). In the autoclave experiments the catalyst activities are measured directly after sulfidation of the catalysts, while in the flow experiments the catalysts were aged during 27 h.

The results of the flow experiments at constant (10 and 50%) HDN-conversions of Q to hydrocarbons are presented in Table 3. At low conversion (10%) the periodic trend of the OPA selectivity of the first-row TMS decreased more or less continuously. Their PCH selectivity followed a shallow U-shaped curve with minimum at Mn/C and

Fe/C, while the PBZ selectivity followed the opposite trend and the PCHE selectivity decreased continuously from group V to group VIII. As a result, Ni/C had the highest PCH and lowest PBZ and PCHE selectivity of the first-row TMS catalysts, that is the highest hydrogenation activity. Also the N-product distribution of the first-row TMS/C catalysts was dependent on the periodic position of the transition metals. The THQ1, DHQ, and THQ5 selectivities followed a U-shaped curve with a minimum at Mn/C and Fe/C and a maximum at Ni/C. The Ni/C catalyst had therefore the highest selectivity for N-compounds with a saturated benzene ring (DHQ and THQ5) as well as a saturated heterocyclic ring (THQ1). The reverse was true for the Mn/C and Fe/C catalysts.

Since the Rh/C catalyst had a very high activity (Table 2) it proved impossible to decrease its conversion to 50% with our present reactor set-up. On the one hand, no reproducible results could be obtained when

lowering the amount of catalyst in the catalyst–SiC mixture below 0.1 g, and on the other hand the maximum space velocity was limited by the fact that the ratio of liquid feed to H_2 had to be kept constant and that the maximum H_2 flow was limited by the mass flow controller range. Therefore only Mo/C, Ru/C, and Pd/C were compared at the 10% conversion level (Table 3). The trends for these three second-row TMS were different from those of the first-row TMS. The OPA selectivity and the production of N-containing byproducts decreased continuously from Mo/C to Pd/C (Table 3). The Mo/C catalyst had the highest cracking and isomerization activity of all second-row TMS. The selectivity for saturated hydrocarbons (PCH) increased and that for unsaturated hydrocarbons (PBZ, PCHE) decreased from Mo/C to Pd/C. Just like in the autoclave experiments, Ru/C had the highest selectivity for DHQ. The THQ5 selectivity increased and the THQ1 selectivity and the residual amount of Q decreased from Mo/C to Pd/C.

The differences between the performances of the third-row TMS catalysts were so large that we were unable to compare the selectivities of all five TMS at the same conversion. At 10% conversion only W/C and Re/C and at 50% conversion only W/C, Re/C, and Os/C could be measured. Os/C, Ir/C, and Pt/C could be measured at 90% conversion, but a comparison of selectivities at this high conversion level is not meaningful. As with the second-row Mo/C catalyst, W/C had the highest selectivity for byproducts of the third-row TMS. In agreement with the autoclave experiments the W/C and Os/C catalysts had very high OPA selectivities and the Re/C catalyst had a very low OPA and high DHQ selectivity. The selectivity for PCH increased and those for PBZ and PCHE decreased from W/C to Os/C.

The results obtained with the second- and third-row TMS/C catalysts can be summarized as follows. At low conversions the yields of Q and THQ1 decrease and those of THQ5, DHQ, and OPA increase with conversion, while at high conversion the yields of all N-containing reactants and intermediates decrease. The yields of all three hydrocarbon products increase with conversion, but the selectivity to PCH increases and those to PCHE and PBZ decrease with conversion. When plotted as a function of conversion the various yields and selectivities of all catalysts adhere more or less to the same curves (Fig. 6). This means that the ratios of all rate constants do not change greatly when going from one TMS/C catalyst to the other. What happens if one goes from one catalyst to the other is that all rate constants change in the same direction. This explains why the periodic trends observed for the overall Q–HDN reaction were equal to those observed for the HDN of intermediates, such as DHQ, CHA, and OPA. As the flow results show, there are differences between the various catalysts. These differences seem to be mainly related to the (de)hydrogenating properties of the catalysts, which increase from left to right in the second and third row. Thus, the PCHE and OPA selectivities decrease, while those of PCH and THQ5 increase from Mo to Pd.

Although our studies have provided a wealth of information about the abilities of the various TMS to hydrodenitrogenate N-containing molecules, further work is needed to evaluate the real prospects of the most promising candidates. To that end we will complement the present qualitative conclusions with quantitative kinetic studies over a limited number of the TMS catalysts. Furthermore we will explore the possibilities to improve the HDN properties by putting active TMS catalysts on supports which can assist in the N-removal part of the HDN network through NH_3 elimination.

CONCLUSIONS

Transition metal sulfides proper can catalyze all the reaction steps of the quinoline HDN reaction; namely the hydrogenation of the benzene ring and of the heterocyclic

ring, the ring opening, as well as the nitrogen removal. The first-row TMS have low Q-conversions to hydrocarbons which, when plotted versus the periodic position of the TMS, form a U-shaped curve with a minimum at Mn/C and Fe/C, and with V/C, Co/C, and Ni/C having the highest conversions. The Q-conversions to hydrocarbons of the second- and third-row TMS form volcano curves with maxima at Rh/C and Ir/C, respectively. Mo/C and W/C had the lowest conversions in these rows. The Q-conversion to hydrocarbons increased from the first row to the second row and to the third-row TMS. The first-row TMS and also Mo/C and W/C had a rather low Q-conversion to hydrocarbons as the formation of DHQ as well as its conversion to hydrocarbons were slow. The TMS with the highest Q-conversion to hydrocarbons (Rh/C, Os/C, and Ir/C) had much higher activities for both reactions. For Ru/C, Pd/C, Re/C, and Pt/C the ratio of the rates for DHQ conversion to hydrocarbons and the formation of DHQ was smaller than for the other catalysts. Re/C and Ru/C have a selectivity to PBZ higher than that of the other TMS with high Q-conversion to hydrocarbons.

REFERENCES

1. Sudhakar, C., Eijsbouts, S., de Beer, V. H. J., and Prins, R., *Bull. Soc. Chim. Belg.* **96,** 885 (1987).

2. Eijsbouts, S., Sudhakar, C., de Beer, V. H. J., and Prins, R., *J. Catal.* **127,** 605 (1991).
3. Eijsbouts, S., de Beer, V. H. J., and Prins, R., *J. Catal.* **109,** 217 (1988).
4. Ledoux, M. J., and Djellouli, B., *J. Catal.* **115,** 580 (1989).
5. Vit, Z., and Zdražil, M., *J. Catal.* **119,** 1 (1989).
6. Pecoraro, T. A., and Chianelli, R. R., *J. Catal.* **67,** 430 (1981).
7. Vissers, J. P. R., Groot, C. K., van Oers, E. M., de Beer, V. H. J., and Prins, R., *Bull. Soc. Chim. Belg.* **93,** 813 (1984).
8. Ledoux, M. J., Michaux, O., Agostini, G., and Pannisod, P., *J. Catal.* **102,** 275 (1986).
9. Zdražil, M., *Appl. Catal.* **4,** 107 (1982).
10. Vrinat, M. L., *Appl. Catal.* **6,** 137 (1983).
11. Schulz, H., Schon, M., and Rahman, N. M., *Stud. Surf. Sci. Catal.* **27,** 201 (1986).
12. Satterfield, C. N., and Cochetto, J. F., *Ind. Eng. Chem. Process Des. Dev.* **20,** 53 (1981).
13. Gioia, F., and Lee, V., *Ind. Eng. Chem. Process Des. Dev.* **20,** 49 (1986).
14. Satterfield, C. N., and Gültekin, S., *Ind. Eng. Chem. Process Des. Dev.* **20,** 62 (1981).
15. Satterfield, C. N., and Yang, S. H., *Ind. Eng. Chem. Process Des. Dev.* **23,** 11 (1984).
16. Yang, S. H., and Satterfield, C. N., *Ind. Eng. Chem. Process Des. Dev.* **23,** 20 (1984).
17. Satterfield, C. N., and Smith, C. M., *Ind. Eng. Chem. Process Des. Dev.* **25,** 942 (1986).
18. Lacroix, M., Boutarfa, N., Guillard, C., Vrinat, M., and Breysse, M., *J. Catal.* **120,** 473 (1989).
19. La Vopa, V., and Satterfield, C. N., *J. Catal.* **110,** 375 (1988).
20. Cocchetto, J. F., and Satterfield, C. N., *Ind. Eng. Chem. Process Des. Dev.* **20,** 49 (1981).
21. Perot, G., Brunet, S., Canaff, C., and Toulhoat, H., *Bull. Soc. Chim. Belg.* **96,** 865 (1987).
22. Gnofam, N., Vivier, L., Brunet, S., Lemberton, J. L., and Perot, G., *Catal. Lett.* **2,** 81 (1989).
23. Levenspiel, O., "Chemical Reaction Engineering," p. 191, Wiley, New York, 1972.
24. Knözinger, H., and Ratnasamy, P., *Catal. Rev. Sci. Eng.* **17,** 31 (1978).